Markov Modulated Process to Model Human Mobility

Markov Modulated Process to model human mobility

Brian Chang[1], Liufei Yang[1], Mattia Sensi[1], Massimo A. Achterberg[1], Fenghua Wang[1], Marco Rinaldi[1], and Piet Van Mieghem[1]

Delft University of Technology, Delft 2628 CD, The Netherlands,
m.sensi@tudelft.nl

Abstract. We introduce a Markov Modulated Process (MMP) to describe human mobility. We represent the mobility process as a time-varying graph, where a link specifies a connection between two nodes (humans) at any discrete time step. Each state of the Markov chain encodes a certain modification to the original graph. We show that our MMP model successfully captures the main features of a random mobility simulator, in which nodes moves in a square region. We apply our MMP model to human mobility, measured in a library.

Keywords: Markov modulated process, human mobility, time-varying networks, modeling, Markov chains

1 Introduction

Over the last century, scientists have modeled the spread of infectious diseases in a population with various approaches and assumptions. Any epidemic outbreak consists of two processes: the viral process describes the transmission of the virus between two hosts and the mobility process specifies when two hosts are in contact for a sufficiently long time at a sufficiently short distance to enable the viral transmission. Since measurements of human mobility were seldom available in earlier times, human mobility has largely been ignored or absorbed into the viral process through time-varying infection and curing probabilities or by imposing restrictions on the contact graph. Simple epidemic models, which do not take mobility into account and consider fixed and static contact networks over time, cannot explain the prolonged duration of an epidemic such as COVID-19 [21].

Recently, various approaches have been proposed to model human mobility [1,5,13,14,16,17,23] and specific aspects such as community and motif formation [15,26] and the movement behavior of each individual [7,18]. Mobile devices are increasingly used to measure movement [8,9,10,17,27]. The impact of human mobility on the spread of epidemics is studied in [2,11,12,19,24,27].

In this paper, we propose a novel approach to the modeling of Human Mobility Processes (HMP)[1] based on a Markov Modulated Process (MMP) [6][22, Sec.

[1] This paper is a abridgement of the master theses of B. Chang [4] and L. Yang [25].

5.2]. Each state of the Markov chain in the MMP encodes an action, which creates a contact graph. For example, state i may generate an Erdős-Rényi graph $G_{p_i}(N)$ with link density p_i, state j may add j links and state k removes a motif (e.g. a triangle) and so on. We evaluate the MMP performance first assuming that nodes move randomly around in a square region and are in contact if their distance is smaller than a certain threshold. We then reconstruct the time-varying contact network using a MMP model.

The paper is structured as follows: Section 2 describes a random mobility simulator. Section 3 briefly introduces Markov Modulated Processes (MMPs) and Section 3.2 compares our MMP model to the mobility simulator. We apply our model to real-world data in Section 4. Finally, we conclude in Section 5.

2 Random mobility simulator

Movements over time are first simulated by a very simple random model, merely to explain and evaluate the idea of a MMP in Section 3. Later, in Section 4, human mobility is measured in a library.

We simulate[2] a mobility process in which nodes are constrained to move within a square region of size $Z \times Z$ units. We consider $N = n^2$ nodes. Initially, the N nodes are spaced evenly at a distance of $Z/(n+1)$ in a square lattice with n rows and n columns. The distance between the edges of the lattice and the border of the region is also $Z/(n+1)$. Figures 1a and 1b show a visualization of the initial placement and a snapshot of a typical realization. The position of each node is represented in Cartesian coordinates (x, y), with the bottom-left corner of the square as origin $(0, 0)$.

The positions of the nodes change at discrete time steps. At time $k = 0$, each node is initialized with a random direction or angle, which is a random integer, uniformly chosen in the range $[0, 359]$. For all remaining time steps, we fix a value $\theta \in (0, 180)$ and each node can change its direction by an integer in the range $[-\theta, \theta]$ with uniform probability. Each node then moves forward in a straight line along its current direction. The move distance is uniformly distributed in the range $[0, 2v]$. We constrain the movement of the nodes to the square region of size $Z \times Z$. If a node attempts to move out of bounds, its x and y coordinates are both clamped to the range $[0, Z]$, bringing the node back into the region. Then, the direction of the node is reset to point towards the center of the region, i.e. the point $(Z/2, Z/2)$. Finally, a random integer offset in the range $[-\phi, \phi]$ is applied to the new direction of the node.

At each discrete time step $k \in \{0, 1, \ldots, T-1\}$, every node moves according to the procedure described above. After the nodes have moved, at $k + 1$, we create a network based on the current positions of the nodes. Two nodes are connected when the distance between them is d units or less; here $d = 1.5$. The temporal contact network $G(N, k)$ is represented by the time-varying $N \times N$

[2] The Python code of our mobility simulator is available on GitHub: https://github.com/twente/mmp-mobility-model

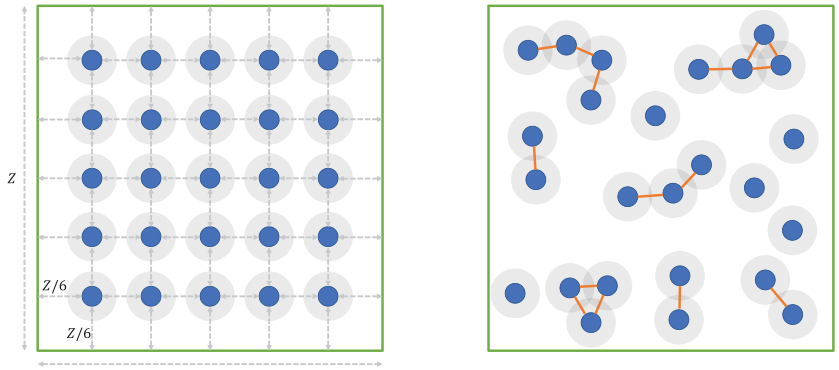

(a) Initial setup of the mobility simulator. (b) Snapshot of one realization.

Fig. 1: Visualization of our random mobility simulator at time $k = 0$ and at another time $k > 0$. If the grey circles around two nodes overlap, a link (shown in orange) between the two is created. The grey circles have radius $d/2 = 0.75$.

adjacency matrix $A(k)$ at discrete time k. Each element $a_{ij}(k) = 1$ if node i and node j are in contact at time k; otherwise, $a_{ij}(k) = 0$.

In the mobility process simulations, we choose $N = 25$ nodes, $Z = 10$ for the size of the region and, further, $\theta = 20$, $v = 1$, $\phi = 30$. We perform 1000 realizations of the mobility process and each realization of the simulated mobility process runs for $T = 1000$ time steps and generates $A(1), A(2), \ldots, A(1000)$ adjacency matrices of contact graphs, starting from an empty initial adjacency matrix $A(0) = O$ at time $k = 0$, representing the evenly-spaced square lattice[3]. Figure 2 illustrates the number of links at each time step for one realization of the mobility process. After performing 1000 realizations of 1000 time steps each in the mobility simulations, Figure 3 plots the distribution of the number of links in the graph at each time step and the number of links added or removed between two time steps.

3 The Markov Modulated Process (MMP)

We consider a temporal graph $G(N, k)$, where the links in the graph change over time, controlled by a discrete-time Markov process. In each state of the Markov chain, an action is executed to modulate the graph. The evolution of the Markov process is controlled by the $M \times M$ probability transition matrix P, whose elements p_{ij} represent the probability of transitioning from state i to state j. The goal is to use a discrete-time Markov process to modulate a time-varying

[3] The spacing in the lattice is $10/6 \approx 1.667$ which exceeds $d = 1.5$; therefore, there are no links in the initial graph at $k = 0$.

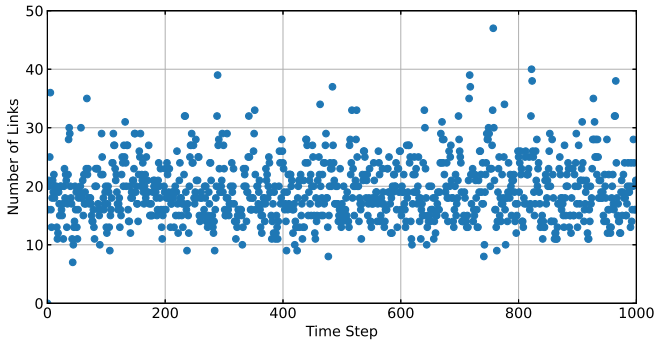

Fig. 2: Number of links at each time step for one realization of the mobility process with $N = 25$ nodes.

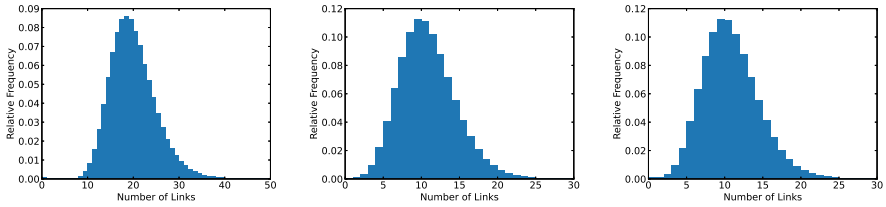

(a) Total number of links. Average: 19.430.

(b) Number of added links. Average: 10.369.

(c) Number of removed links. Average: 10.350.

Fig. 3: Histograms of link statistics for the simulated mobility process with 25 nodes across 1000 realizations of 1000 time steps.

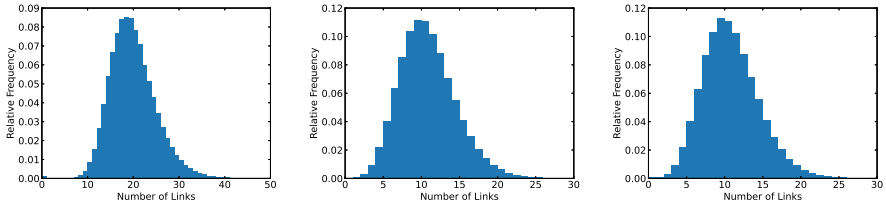

(a) Total number of links. Average: 19.433.

(b) Number of added links. Average: 10.369.

(c) Number of removed links. Average: 10.350.

Fig. 4: Histograms of link statistics for the reduced MMP model with 25 nodes across 1000 realizations of 1000 time steps.

graph of 25 nodes, such that the series of MMP generated adjacency matrices has properties which closely resemble those of the series of adjacency matrices produced by the mobility process.

3.1 A first approach: the combinatorial MMP model

Between two consecutive time steps of the mobility process, links in the contact graph are both added and removed. In order for the average number of links over time in the MMP model to match the mobility process, a feedback mechanism is needed to control the number of links. Without feedback, the MMP model does not track the number of links, which will consequently drift like a random walk over time [25, Sec. 3.5]. Therefore, the states of the MMP model should encode the number of links in the graph at each discrete time step.

In the first approach, each state of the Markov process represents the number of links in the graph as well as a modulating action f which will be applied to the temporal graph. The action $f = (+a, -b)$ consists of randomly adding a links and removing b. The set of possible actions is bounded by the number of links which currently exist in the graph, because we cannot remove more links than currently exist nor add more links than can be accommodated by the complete graph. Given that i links currently exist in the graph, the *complete action set* J_i is the set of all possible actions, given by

$$J_i := \{f = (+a, -b) | 0 \leq a \leq L_{\max} - i, 0 \leq b \leq i\}, \tag{1}$$

where $L_{\max} = \binom{N}{2} = N(N-1)/2$ is the number of links in the complete graph with N nodes. Given i links in the graph, there are thus $(i+1)(L_{\max} - i + 1)$ possible actions, each of which will be encoded by a state in the MMP model. As an example, consider $N = 3$ nodes. Since $L_{\max} = 3$, the complete action sets for each possible number of links is:

$$\begin{aligned}
J_0 &= \{(+0, -0), (+1, -0), (+2, -0), (+3, -0)\}, \\
J_1 &= \{(+0, -0), (+0, -1), (+1, -0), (+1, -1), (+2, -0), (+2, -1)\}, \\
J_2 &= \{(+0, -0), (+0, -1), (+0, -2), (+1, -0), (+1, -1), (+1, -2)\}, \\
J_3 &= \{(+0, -0), (+0, -1), (+0, -2), (+0, -3)\}.
\end{aligned}$$

For each of the complete action sets, every action is assigned to a unique state. Hence, the same action can appear multiple times, but for a different number of links. The Markov states, numbered arbitrarily in format $S_n : \{L, f\}$, where L is the number of links currently in the graph, for the example of $N = 3$ are:

$$\begin{array}{cccc}
S_1 : \{0, (+0, -0)\} & S_2 : \{0, (+1, -0)\} & S_3 : \{0, (+2, -0)\} & S_4 : \{0, (+3, -0)\} \\
S_5 : \{1, (+0, -0)\} & S_6 : \{1, (+0, -1)\} & S_7 : \{1, (+1, -0)\} & S_8 : \{1, (+1, -1)\} \\
S_9 : \{1, (+2, -0)\} & S_{10} : \{1, (+1, -2)\} & S_{11} : \{2, (+0, -0)\} & S_{12} : \{2, (+0, -1)\} \\
S_{13} : \{2, (+0, -2)\} & S_{14} : \{2, (+1, -0)\} & S_{15} : \{2, (+1, -1)\} & S_{16} : \{2, (+1, -2)\} \\
S_{17} : \{3, (+0, -0)\} & S_{18} : \{3, (+0, -1)\} & S_{19} : \{3, (+0, -2)\} & S_{20} : \{3, (+0, -3)\}
\end{array}$$

With the states of the MMP model now defined, the next step is to construct the probability transition matrix P from the mobility process. At each time step $k < T$ of the mobility process, the number of links in the adjacency matrix $A(k+1)$ is compared with $A(k)$ to determine how many links to add and remove

(i.e. the action). The number of links and the action allow us to determine the Markov state at time k. The transition probability,

$$p_{ij} = \frac{n_{ij}}{\sum_{m \in X} n_{im}}, \tag{2}$$

equals the number n_{ij} of observed transitions from state i to state j divided by the total number of observed transitions from state i to any other state m, where X is the set of all states.

Because each state $S_n : \{L, f\}$ of the combinatorial MMP model encodes both the number of links in the graph as well as an action, the total number M of states is found by summing the number of possible actions over all possible numbers of links which can exist in the graph, $M = \sum_{i=0}^{L_{\max}} (i+1)(L_{\max} - i + 1)$ which is $M = \mathcal{O}(N^6)$ as shown in [25, Sec. 4.2]. As the size N of the graph increases, the computational complexity of the combinatorial MMP model quickly explodes and becomes infeasible.

3.2 Reduced MMP model for human mobility

The computational intractability has led us to simplify the combinatorial MMP model in Section 3.1 to a *reduced MMP model*, in which each state $\{0, 1, \ldots, L_{\max}\}$ represents the number of links in the graph and not a specific action. The number of states required is therefore $M = L_{\max} + 1 = \mathcal{O}(N^2)$, since one additional state is required for the null graph with 0 links. A Markov state is assigned to each time step $k \leq T$ of the mobility process and the state corresponds to the number of links in the adjacency matrix $A(k)$. The transition probabilities of the probability transition matrix P are then calculated by (2).

The actions of the reduced MMP model are no longer embedded in the states, and instead we define a *transition action set* J_{ij} for each state transition from state i to j. Each transition action set J_{ij} will be a subset of the corresponding complete action set J_i that was described in (1). The transition action set J_{ij} is defined as the set of possible actions, given that i links currently exist in the graph, that will result in j links after the action is applied, and expressed as

$$\begin{aligned} J_{ij} :=& \{f = (+a, -b) | j - i = a - b, 0 \leq a \leq L_{\max} - i, 0 \leq b \leq i\} \\ =& \{f \in J_i | j - i = a - b\}. \end{aligned} \tag{3}$$

Revisiting the example of $N = 3$ nodes, the transition action sets are given by:

$$\begin{array}{llll} J_{00} : \{(+0, -0)\} & J_{01} : \{(+1, -0)\} & J_{02} : \{(+2, -0)\} & J_{03} : \{(+3, -0)\} \\ J_{10} : \{(+0, -1)\} & J_{11} : \{(+0, -0), (+1, -1)\} & J_{12} : \{(+1, -0), (+2, -1)\} & J_{13} : \{(+2, -0)\} \\ J_{20} : \{(+0, -2)\} & J_{21} : \{(+0, -1), (+1, -2)\} & J_{22} : \{(+0, -0), (+1, -1)\} & J_{23} : \{(+1, -0)\} \\ J_{30} : \{(+0, -3)\} & J_{31} : \{(+0, -2)\} & J_{32} : \{(+0, -1)\} & J_{33} : \{(+0, -0)\} \end{array}$$

When we transition from state i to state j in the reduced MMP model, we select an action f from the corresponding transition action set J_{ij} with probability $\Pr[J_{ij}(f)] = \frac{n(f)_{ij}}{n_{ij}}$, where $n(f)_{ij}$ is the number of times action f is observed

during transitions from i links to j links in the mobility process and n_{ij} is the total number of observed transitions from i to j links.

The probability distribution of the transition action set is independent of the transition probabilities of the Markov process. The probability of an action $f \in J_{ij}$, given that there are currently i links in the graph, is given by $p_{ij} \Pr[J_{ij}(f)]$, which is the probability of transitioning from i to j links multiplied by the probability of choosing action f from J_{ij}. The probability of each action is only dependent on the current number of links in the graph: by the Markov property, the next state depends only on the current state (i.e. the current number of links) and the probability distribution of each action set is fixed.

The reduced MMP model can be directly derived from the combinatorial MMP model as shown in [25, Sec. 4.3]. Both MMP models will produce [25] a modulated graph with the same number of links on average and the long-term rate at which each action is applied is the same for both models. The dependence between consecutive actions is lost in the reduced MMP model: the combinatorial MMP model embeds the actions in the Markov states, and hence the probability of the next action has a dependence on the previous action. In the reduced MMP model, the next action is dependent only on the current number of links. If, in the mobility process being modeled, there is a negligible amount of dependence between consecutive actions, then the combinatorial MMP model is actually trying to model a dependence that does not exist. Therefore, no information is lost in the reduced MMP model, as is the case in our simulated mobility process [25, Sec. 5.5]. The reduced MMP model in Figure 4 is extremely close to simulated mobility in Figure 3.

In Figure 5, we plot for the two processes the *K-step link retention probability*, which is the probability [20, p. 182] that a link still exists at time $k+K$, given that the link existed at the time k. For the MMP models, the link retention probability decreases exponentially [20, p. 182] in K. Figure 4 indicates that the probability that a link is not removed is approximately $1 - (10.350/19.433) \approx 0.47$. Since the removed links are chosen randomly, we expect an exponential decay of the K-step retention probability. Compared to the mobility process, however, the link retention probability of the MMP models is lower for larger steps. Although Figures 3 and 4 are almost indistinguishable, the link retention probabilities of the MMP model and the mobility process start to deviate after 3 time steps. This prompts further research of the algorithm which selects the links to be added and removed at each time step.

4 Real-world application of MMP to HMP in a library

The mobility data was recorded in the TU Delft library during a single day from 08:00 to 18:00. In the tracking experiment, each of the 37 participants wears a Bluetooth tracking device and there are fixed Bluetooth beacons inside the library. Each Bluetooth tracking device will record contact events with beacons, and each data record includes the time and duration of the contact, the distance from the beacon and information to uniquely identify the device and beacon.

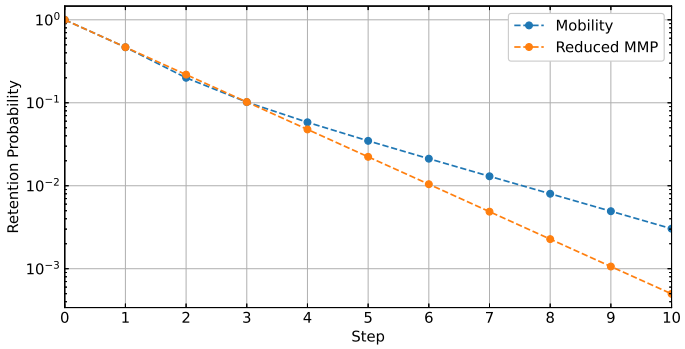

Fig. 5: Comparison of the K-step link retention probability between the mobility process and the reduced MMP model. The two curves remain really close up to step 3, whereafter they start to diverge.

4.1 Building the reduced MMP Model

The tracking devices record the contacts between people every 30 seconds. The opening time of the library at 08:00 is set at $k = 0$ and the closing time at 18:00 at time $k = 1200$. The adjacency matrix $A(k)$ represents the contact graph at discrete time $k \in [0, 1200]$.

We plot the number of links at each time step in Figure 6. We observe that there are almost no contacts, except for the two spikes in the number of contacts, from 11:04 to 12:54 and from 15:10 to 16:20.

Since our MMP model is based on the number of links in the graph, we focus on modeling the first spike in contacts from 11:04 to 12:54, corresponding to time step $k = 369$ to $k = 587$; this time window is highlighted by a yellow stripe in Figure 6. We compute the total number of links at each time step (average is 2.84) and the number of links added (average is 0.11) and removed (average is 0.11) between two time steps. We use the adjacency matrices to generate the probability transition matrix and build the action sets. The mobility process runs for a little over 200 time steps, so we choose to simulate the MMP model for 200 time steps; the number of realizations is kept at 1000 as previously.

4.2 Results of the reduced MMP Model

The maximum number of links in a graph of 37 nodes is $\binom{37}{2} = 666$ and the reduced MMP model needs $M = 667$ states. However, Figure 6 shows that a maximum of 9 links was observed. For $M = 10$ states, there are 100 possible state combinations, but we only observed 27 transitions; so we consider 27 action sets.

In each realization, the Markov process is initialized in state 0 with an empty graph. After performing 1000 simulations of 200 time steps, we calculate the total

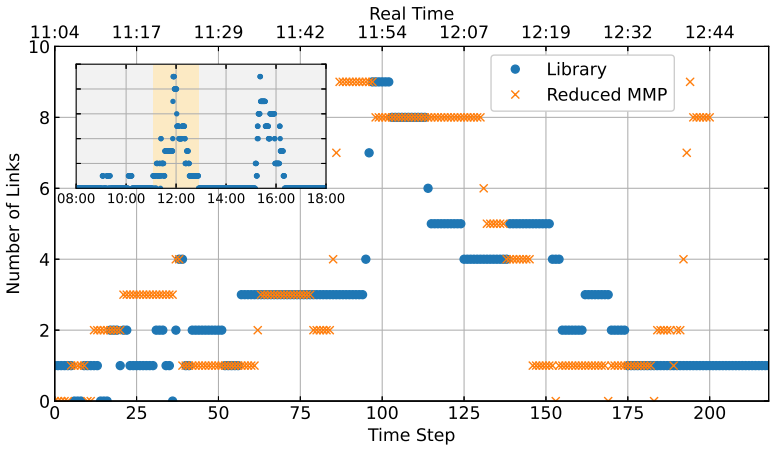

Fig. 6: Number of links at each time step for the mobility process in the library (blue circles) and for a realization of our reduced MMP model (orange crosses). The time steps of our chosen window have been re-indexed to start from 0. Inset: entire data from the recorded day, the yellow strip represents the time window which is modeled by the MMP model.

number of links at each time step (average 2.607) and the number of links added (average 0.120) and removed (average 0.106) between two time steps. In the MMP model, the average number of links observed at each time step is about 8.3% lower compared to the library mobility process. The average number of links added is about 8.9% higher, and the average number of removed links is about 3.7% lower. The error of the MMP model for the library data is relatively large compared to the random mobility simulator. We attribute this large difference to the fact that the number of links in the graph is small and that the model is run for fewer time steps.

One immediate observation is that the real mobility process in Figure 6 exhibits a pronounced increase in the number of links followed by a decrease, but this trend is not captured by the MMP model. Figure 6 reveals that the modulated graph reaches 9 links at $t = 87$ and remains there until $t = 97$. At $t = 98$, the MMP then transitions to 8 links and remains there for until $t = 130$. To better understand this behavior, we investigate the probability transition matrix of the MMP model in Figure 7.

Row i of the transition matrix P in Figure 7 corresponds to state i, which encodes i links in the graph. Hence, the entry (i, j) indicates the probability of having j links in the graph after the next action. The 9th row in Figure 7 indicates an 83% probability of staying at 9 links and a 17% probability of transitioning to 8 links. This probability is derived by observing the number of links in the mobility process in Figure 6. From time $k = 97$ to $k = 102$, the graph has 9 links. This means that we observe 5 transitions from 9 links to 9

	0	1	2	3	4	5	6	7	8	9
0	0.57	0.14	0.29	0.00	0.00	0.00	0.00	0.00	0.00	0.00
1	0.04	0.90	0.04	0.01	0.00	0.00	0.00	0.00	0.00	0.00
2	0.00	0.16	0.77	0.03	0.03	0.00	0.00	0.00	0.00	0.00
3	0.00	0.00	0.02	0.96	0.02	0.00	0.00	0.00	0.00	0.00
4	0.00	0.05	0.05	0.00	0.80	0.05	0.00	0.05	0.00	0.00
5	0.00	0.00	0.00	0.00	0.09	0.91	0.00	0.00	0.00	0.00
6	0.00	0.00	0.00	0.00	0.00	1.00	0.00	0.00	0.00	0.00
7	0.00	0.00	0.00	0.00	0.00	0.00	0.00	0.00	0.00	1.00
8	0.00	0.00	0.00	0.00	0.00	0.00	0.09	0.00	0.91	0.00
9	0.00	0.00	0.00	0.00	0.00	0.00	0.00	0.00	0.17	0.83

Fig. 7: Probability transition matrix P of the MMP model based on the real mobility process.

links. At $k = 103$, the graph transitions to 8 links and for the remainder of the mobility process, we never observe 9 links in the graph again. We observed no transition from 9 links to a number of links different from 8 and 9. Therefore, the probabilities in the probability transition matrix are $1/6 \approx 0.17$ and $5/6 \approx 0.83$, respectively.

Due to the limited amount of data, the MMP model is sensitive to the idiosyncrasies of this particular dataset and the model overfits the data. Consider how state 9 can be reached: from the probability transition matrix, we observe that the only way to reach state 9 is from state 7 and the corresponding transition probability is 1. The original mobility process, in contrast, is interpreted as follows: the only way for 9 contacts between people occurs if there were 7 contacts between them 30 seconds ago (one time step). Furthermore, if there are currently 7 contacts between people, there is a 100% probability that after 30 seconds, there will be 9 contacts. The MMP model only incorporates transitions that have been observed in the mobility process. Unobserved transitions in the real mobility process have zero probability in the MMP model.

5 Conclusions and outlook

We present the idea of a Markov Modulated Process (MMP) for constructing temporal contact networks for human mobility. The states of our reduced MMP model encode the number of links in the graph. We illustrate the accuracy of the MMP model for both a random mobility simulator and for real-world movements in a library. Surely, our implementation of a MMP can be improved.

A first concern is the overfitting of the current MMP model. Only observed transitions in the mobility process may occur in the MMP model. Any other transition is impossible, even though such transition may be possible in reality. The MMP model can be improved by data augmentation of the mobility process, especially regarding rare events [3].

Another challenge is to encode spatial correlations in the MMP model. The *number of* added and removed links in the graph is based on the MMP model,

but *which* link should be removed is currently random. Thus, spatial correlation between the nodes is ignored in the current implementation and we propose to adjust the reduced MMP model to incorporate the spatial correlations.

A third drawback of the reduced MMP model is that we implicitly assume that the number of links in the network is roughly constant. Practical situations for modeling population flow, such as airports, schools, libraries and other transfer locations, typically show activity spikes around certain events, such as lunch time. The reduced MMP formulation performs well in situations where activity stays roughly constant, such as long-term interactions of individuals with friends and family, but does not capture activity spikes.

We believe that Markov Modulated Processes constitute a powerful framework for modeling human mobility and may ultimately ameliorate the models for investigating the spread of infectious diseases.

Acknowledgements: The authors thank Dr. ir. Sascha Hoogendoorn-Lanser for sharing the library data, which has been collected as part of an ongoing project led by her at TU Delft.

References

1. Barbosa, H., Barthelemy, M., Ghoshal, G., James, C. R., Lenormand, M., Louail, T., Menezes, R., Ramasco, J. J., Simini, F., Tomasini, M.: Human mobility: Models and applications (2018). Physics Reports, 734, 1-74.
2. Barmak, D. H., Dorso, C. O., Otero, M.: Modelling dengue epidemic spreading with human mobility (2016). Physica A: Statistical Mechanics and its Applications, 447, 129-140.
3. Causer, L., Carmen Bañuls, M., Garrahan, J.P.: Optimal sampling of dynamical large deviations via matrix product states. PRE 103, 062144 (2021).
4. Chang, B.: Modeling the Spread of Epidemics (2021), MSc. Thesis, Delft, University of Technology, http://resolver.tudelft.nl/uuid:72206da3-4652-4a10-90bd-2fdd2a1e98f6
5. Feng, J., Yang, Z., Xu, F., Yu, H., Wang, M., Li, Y.: Learning to simulate human mobility (2020). In Proceedings of the 26th ACM SIGKDD International Conference on Knowledge Discovery & Data Mining (pp. 3426-3433).
6. Fischer, W., Meier-Hellstern, K.: The Markov-modulated Poisson process (MMPP) cookbook (1993). Performance Evaluation 18(2) 149-171 (1993). https://doi.org/10.1103/PhysRevE.103.062144
7. Flores, M. A. R., Papadopoulos, F.: Similarity forces and recurrent components in human face-to-face interaction networks (2018). Physical review letters, 121(25), 258301.
8. Hossmann, T., Spyropoulos, T., Legendre, F.: A complex network analysis of human mobility (2011). In 2011 IEEE conference on computer communications workshops (INFOCOM WKSHPS) (pp. 876-881). IEEE.
9. Huang, Z., Ling, X., Wang, P., Zhang, F., Mao, Y., Lin, T., Wang, F. Y.: Modeling real-time human mobility based on mobile phone and transportation data fusion (2018). Transportation research part C: emerging technologies, 96, 251-269.
10. Karamshuk, D., Boldrini, C., Conti, M., Passarella, A.: Human mobility models for opportunistic networks (2011). IEEE Communications Magazine, 49(12), 157-165.

11. Mari, L., Bertuzzo, E., Righetto, L., Casagrandi, R., Gatto, M., Rodriguez-Iturbe, I., Rinaldo, A.: Modelling cholera epidemics: the role of waterways, human mobility and sanitation (2012). Journal of the Royal Society Interface, 9(67), 376-388.
12. Meloni, S., Perra, N., Arenas, A., Gómez, S., Moreno, Y., Vespignani, A.: Modeling human mobility responses to the large-scale spreading of infectious diseases (2011). Scientific reports, 1(1), 1-7.
13. Nguyen, A. D., Sénac, P., Ramiro, V., Diaz, M.: STEPS-an approach for human mobility modeling (2011). In International Conference on Research in Networking (pp. 254-265). Springer, Berlin, Heidelberg.
14. Pappalardo, L., Rinzivillo, S., Simini, F.: Human mobility modelling: exploration and preferential return meet the gravity model (2016). Procedia Computer Science, 83, 934-939.
15. Schneider, C. M., Belik, V., Couronné, T., Smoreda, Z., González, M. C.: Unravelling daily human mobility motifs (2013). Journal of The Royal Society Interface, 10(84), 20130246
16. Solmaz, G., Turgut, D.: A survey of human mobility models (2019). IEEE Access, 7, 125711-125731.
17. Song, C., Koren, T., Wang, P., Barabási, A. L.: Modelling the scaling properties of human mobility (2010). Nature physics, 6(10), 818-823.
18. Starnini, M., Baronchelli, A., Pastor-Satorras, R.: Modeling human dynamics of face-to-face interaction networks (2013). Physical review letters, 110(16), 168701.
19. Tizzoni, M., Bajardi, P., Decuyper, A., Kon Kam King, G., Schneider, C. M., Blondel, V., Smoreda, Z., González, M. C., Colizza, V.a: On the use of human mobility proxies for modeling epidemics (2014). PLoS computational biology, 10(7), e1003716.
20. Van Mieghem, P.: Performance analysis of complex networks and systems (2014). Cambridge University Press.
21. Van Mieghem, P., Achterberg, M.A., Liu, Q.: Power-law decay in epidemics is likely due to interactions with the time-variant contact graph (2020). Delft University of Technology, report20201201, available online at https://nas.ewi.tudelft.nl/people/Piet/TUDelftReports.html
22. Van Mieghem, P., Steyaert, B., Petit, G. H.: Performance of cell loss priority management schemes in a single server queue (1997). International Journal of Communication Systems, 10(4), 161-180.
23. Wang, J., Kong, X., Xia, F., Sun, L.: Urban human mobility: Data-driven modeling and prediction (2019). Acm Sigkdd Explorations Newsletter, 21(1), 1-19.
24. Wesolowski, A., Eagle, N., Tatem, A. J., Smith, D. L., Noor, A. M., Snow, R. W., Buckee, C. O.: Quantifying the impact of human mobility on malaria (2012). Science, 338(6104), 267-270.
25. Yang, L.: Developing a Markov-Modulated Process Model for Mobility Processes (2021), MSc. Thesis, Delft, University of Technology, http://resolver.tudelft.nl/uuid:d37a389d-4145-4ebd-95fc-3dbe351158ad
26. Yang, S., Yang, X., Zhang, C., Spyrou, E.: Using social network theory for modeling human mobility (2010). IEEE network, 24(5), 6-13.
27. Zhou, Y., Xu, R., Hu, D., Yue, Y., Li, Q., Xia, J.: Effects of human mobility restrictions on the spread of COVID-19 in Shenzhen, China: a modelling study using mobile phone data (2020). The Lancet Digital Health, 2(8), e417-e424.